

# Labeling studies of photolabile philanthotoxins with nicotinic acetylcholine receptors: mode of interaction between toxin and receptor

Seok-Ki Choi<sup>1†</sup>, Aristotle G Kalivretenos<sup>1‡</sup>, Peter NR Usherwood<sup>2</sup>  
and Koji Nakanishi<sup>1\*</sup>

<sup>1</sup>Department of Chemistry, Columbia University, New York, NY 10027, USA and <sup>2</sup>Department of Life Science, University of Nottingham, Nottingham, NG7 2RD, UK

**Background:** The nicotinic acetylcholine receptors (nAChRs) and glutamate receptors are ligand-gated cation channels composed of five separate polypeptide chains. A 43 kDa protein of unknown function is non-covalently associated with the cytoplasmic side of nAChR *in vivo*. The venoms of many wasps and spiders contain toxins that block the activity of these channels. Philanthotoxin-433 (PhTX-433) is a non-competitive channel blocker found in the venom of the wasp *Philanthus*. We have used a photolabile derivative to investigate how PhTX-433 interacts with nAChRs.

**Results:** A radiolabeled PhTX analog, containing a photolabile group substituted on one of its aromatic rings, photocrosslinked to all five subunits ( $\alpha$ ,  $\alpha'$ ,  $\beta$ ,  $\gamma$ ,  $\delta$ ) of purified nAChR in the absence of the 43 kDa protein. In the presence of the 43 kDa protein, the  $\alpha$  subunit was

preferentially labeled. Proteolysis of the receptor after crosslinking indicated that the hydrophobic end (head) of the PhTX-433 analog bound to the cytoplasmic loop(s) of the  $\alpha$ -subunit. Binding is inhibited by other non-competitive channel blockers such as the related polyamine-amide toxins from spiders and chlorpromazine.

**Conclusions:** These results, coupled with previous structure/activity studies, lead to a putative model of the binding of PhTx and related polyamine toxins to nAChRs *in vitro*. The 43 kDa protein appears to influence the orientation of toxin binding. Further binding studies are necessary to confirm the model and to define how toxins enter the receptor and how they are oriented within it. A precise understanding of ligand/receptor interaction is crucial for the design of drugs specific for a particular subtype of receptor.

Chemistry & Biology January 1995, 2:23–32

Key words: glutamate receptors, nicotinic acetylcholine receptors, philanthotoxins, photoaffinity labeling, wasp toxin

## Introduction

Many polyamine-amide toxins from funnel-web spider venoms are potent noncompetitive antagonists of neurotransmitter receptors in vertebrate and invertebrate neurons [1,2] (Fig. 1). The venom sac of the parasitic *Philanthus* wasp also contains a similar toxin, philanthotoxin-433 (PhTX-433; the numerals denote number and sequence of methylene groups between amino groups) [3,4] (Fig. 1). These polyamine-amide toxins inhibit conductance of cation channels gated by nicotinic acetylcholine receptors (nAChRs) or ionotropic glutamate receptors (GluRs) [5] located at post-synaptic neurons. Receptors of this type are part of a superfamily of ligand-gated, ion channel receptors which also include serotonin receptors, glycine receptors, and  $\gamma$ -aminobutyric acid (GABA) receptors [6]. The ionotropic GluRs, gated by the neurotransmitter L-glutamate, are some of the principal excitatory amino acid receptors in the vertebrate central nervous system and the invertebrate peripheral nervous system, and have been implicated in learning and memory. It has been suggested that a number of neurodegenerative diseases are caused by alterations in the normal function of these receptors. The

vertebrate GluRs are further divided into two sub-classes based on their responses to exogenous ligands: N-methyl-D-aspartate receptors (NMDA-Rs) and kainate (KAIN)/ $\alpha$ -amino-3-hydroxy-5-methyl-4-isoxazolepropionate (AMPA) receptors (non-NMDA-Rs). The invertebrate GluRs are classified into four subtypes: (i) quisqualate receptors which gate cations (qGlu-R), (ii) ibotenate receptors which gate Cl<sup>-</sup> channels, (iii) a purported KAIN-R, and (iv) a purported NMDA-R.

Previous electrophysiological studies and biochemical binding assays suggest that the polyamine-amide neurotoxins comprise a novel class of non-competitive channel blockers of cation-conducting transmitter receptors in nervous systems [1–5]. Our understanding of the major mode of non-competitive antagonism is that the toxins enter and plug the open cation channels gated by GluR and nAChR, and sterically inhibit the ion flow. But because of the complex properties of polyamines, and the diversity in cellular responses, the interactions between polyamine-amides and channels are not understood at the molecular level. As a first step, the structure-activity relationships of PhTX analogs have been assessed by

\*Corresponding author. †Present address: Department of Chemistry, Harvard University, Cambridge, MA 02138, USA.

‡Present address: Department of Chemistry and Biochemistry, University of Maryland Baltimore County, Maryland, MD 21228, USA.



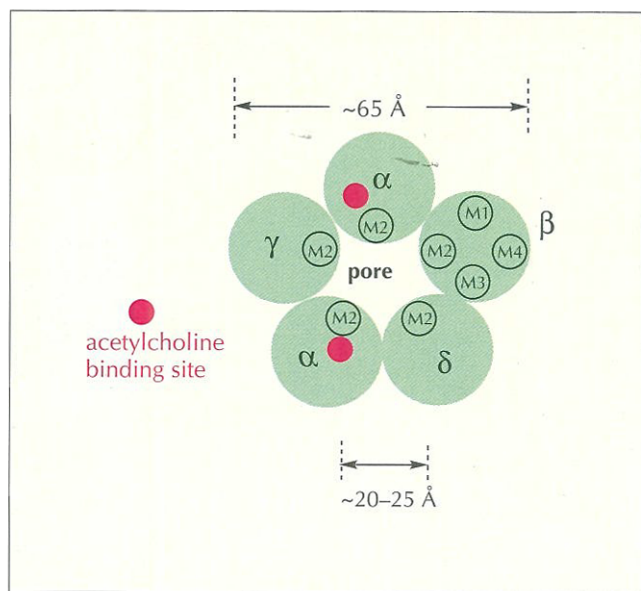


**Fig. 3.** The five subunits of nAChR. Each subunit has four transmembrane segments, M1–M4; the amphiphilic helices, M2, of each subunit line the gate. A further putative helical domain called MA resides in the cytoplasmic region (see Fig. 7b). Binding of acetylcholine to sites within the two  $\alpha$ -subunits opens the channel.

polyamine skeleton rather than the 433 backbone due to ease of synthesis. In the following, the ability of toxins to block ion channels gated by nAChR is presented as relative activity compared to natural PhTX-433 ( $IC_{50}$  for competition with  $^3H$ -perhydrohistrionicotoxin =  $1.1 \mu M$ , relative activity = 1). The relative activity of the analog PhTX-343 is 0.4 times that of native PhTX-433

[8]. Analog 2 contains three modifications to the PhTX-343 structure: first, the precursor is elongated by a Lys residue in region II (this single modification increases the relative activity by a factor of 3.0); second, the photosensitive azido phenyl moiety has been added to region III (the relative activity for analogs carrying only this modification was not measured); and, finally, it is diiodinated in region IV (the relative activity for an analog carrying only this modification is 3.6). The relative activity for analog 2 is 1.3 [8] which is less than that of the analogs containing either of the single modifications for which there are data. Recent results appear to show that when two bulky hydrophobic groups coexist in regions III and IV, the activity of the doubly-modified analog is less than that of each of the component, singly-modified analogs. Analog 2, however, is highly active against qGluR, with a relative activity of 10 [8]. Incorporation of radioactive iodine was accomplished by electrophilic iodination of the Tyr moiety in the last stage of synthesis [24], thus allowing convenient preparation of labeled PhTX with a high specific activity of  $25 \text{ Ci mmol}^{-1}$ .

#### Crosslinking of nAChR subunits

The nAChR antagonist  $N_3\text{Ph-}^{125}\text{I}_2\text{PhTX-343-Lys}$  (analog 2) ( $IC_{50} = 0.84 \mu M$ ,  $25 \text{ Ci mmol}^{-1}$ ) was incubated with  $\alpha$ -cobrotoxin affinity-purified nAChR ( $0.25 \mu M$ ) from *Torpedo californica* [25–29] and irradiated at 254 nm. nAChR was cross-linked with analog 2 in 7–10 % yield, with the two  $\alpha$  subunits and the  $\beta$ ,  $\gamma$  and  $\delta$  subunits labeled with relative intensities of 2.1, 1.0, 0.8 and 1.0, respectively (Fig. 5a, lane 2). Without irradiation, no cross-linking was observed (lane 3), and addition of

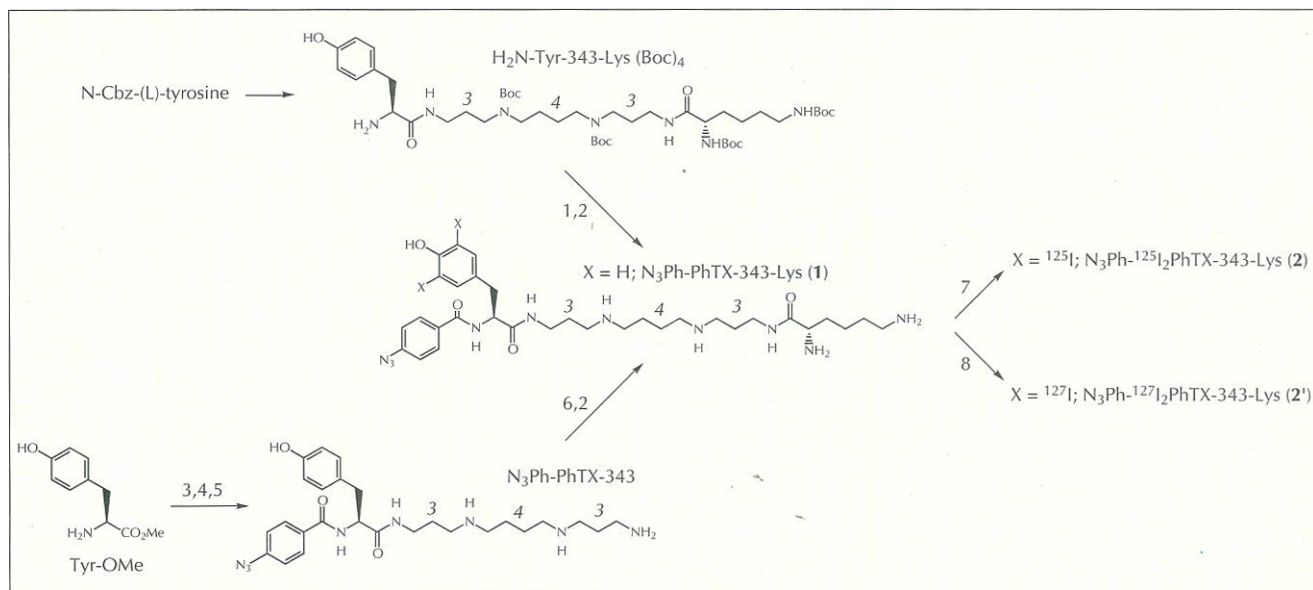


**Fig. 4.** Synthesis of  $N_3\text{Ph-I}_2\text{PhTX-343-Lys}$ . Reagents and conditions: 1) *p*-azidobenzoic acid, diphenylphosphoryl azide (DPPA), dimethyl formamide (DMF), room temperature, 85 %; 2) trifluoroacetic acid/ $\text{CH}_2\text{Cl}_2$  (1/1),  $0^\circ\text{C}$ , 4 h, 90–95 %; 3) *p*-azidobenzoyl chloride,  $\text{Et}_3\text{N}$ ,  $\text{CH}_2\text{Cl}_2$ , 79 %; 4)  $\text{LiOH}$ ,  $\text{MeOH}/1,2\text{-dimethoxyethane (DME)}/\text{H}_2\text{O}$  (3/2/1), room temperature, 95 %; 5) a) 1,3-dicyclohexylcarbodiimide (DCC), *p*-nitrophenol,  $\text{EtOAc}$ , room temperature; b) spermine,  $\text{MeOH}$ , room temperature, 45 %; 6)  $\text{N}^\alpha, \text{N}^\epsilon$ -di-Boc-lysine *p*-nitrophenyl ester, DMF, room temperature, 85 %; 7)  $\text{Na}^{125}\text{I}$ ,  $\text{Na}^{127}\text{I}$ , chloramine-T,  $1 \text{ M K}_2\text{HPO}_4$ , pH 6.0.; 8)  $\text{KI}$ ,  $\text{N-bromosuccinimide (NBS)}$ ,  $\text{K}_2\text{HPO}_4$ ,  $\text{H}_2\text{O}/\text{MeOH}$ , 60–80 %.

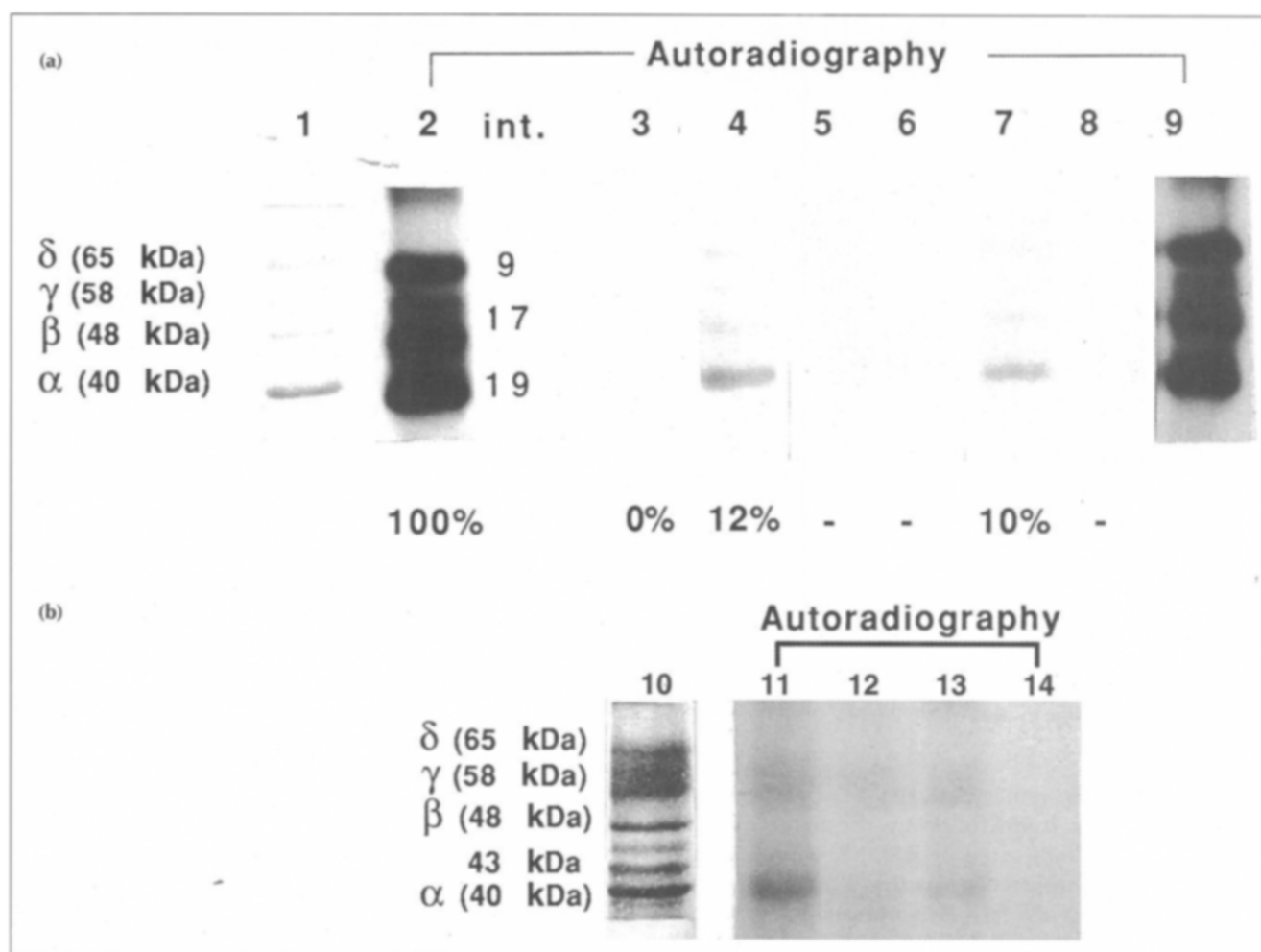


**Fig. 5.** Photoaffinity labeling of nAChR with analog 2. Representative procedure: **(a)** The radioactive  $N_3\text{Ph-}^{125}\text{I}_2\text{PhTX-343-Lys}$  ( $1.90 \mu\text{M}$ ,  $25 \text{ Ci mmol}^{-1}$ ) and non-radioactive effector (as described below) were mixed with *Torpedo* nAChR ( $0.25 \mu\text{M}$ ) purified with  $\alpha$ -cobrotoxin affinity chromatography. After incubation for 30 min at  $4^\circ\text{C}$ , carbamylcholine ( $13 \mu\text{M}$ ) was added to the mixture of toxin/receptor. The resulting mixture was further incubated for 4 h at  $4^\circ\text{C}$ , followed by 20 min UV-irradiation at  $254 \text{ nm}$  at  $4^\circ\text{C}$ . After SDS-PAGE of irradiated nAChR, the dried gel was subject to autoradiography. Lane 1 is a picture of a Coomassie blue stained gel of nAChR. Lanes 2–9 are autoradiograms of gels. Lane 2, control, no addition of non-radioactive effector; lane 3, no UV; lane 4,  $1.25 \text{ mM}$   $N_3\text{Ph-}^{125}\text{I}_2\text{PhTX-343-Lys}$ ; lane 5,  $1.25 \text{ mM}$   $\text{I}_2\text{PhTX-343-Arg}$ ; lane 6,  $1.25 \text{ mM}$   $\text{C10-PhTX-343-Arg}$ ; lane 7,  $1.25 \text{ mM}$   $\text{Me}_2\text{-ArgTX-636}$ ; lane 8,  $1.25 \text{ mM}$  chlorpromazine; lane 9,  $16.7 \mu\text{M}$   $\alpha\text{-BgTX}$ . The relative intensities of labeling are shown at the bottom of each lane and are based on measurements by PhosphorImager® (Molecular Dynamics), in which the dried gel is inserted into a cassette for 4–6 h to avoid saturation of bands. The intensity of the control (lane 2) was taken as 100%; the relative intensities of  $\alpha$ ,  $\beta/\gamma$ , and  $\delta$  subunits are given along the respective bands (19:17:9 or 2.1:1.9:1.0). **(b)** Photoaffinity labeling of nAChR with analog 2 in the presence of the 43 kDa protein. The nAChR/43 kDa enriched membranes ( $0.25 \mu\text{M}$ ) in *Torpedo* saline buffer were photolabeled with  $N_3\text{Ph-}^{125}\text{I}_2\text{PhTX-343-Lys}$  ( $1.4 \mu\text{M}$ ) in the presence of carbamylcholine ( $1 \text{ mM}$ ) and non-radioactive effector as described in (a). Lane 10 is a Coomassie blue stained gel of nAChR/43 kDa. Lanes 11–14 are autoradiograms of gels. Lane 11, control, no addition of non-radioactive effector; lane 12,  $0.8 \text{ mM}$   $\text{C10-PhTX-343-Arg}$ ; lane 13,  $0.8 \text{ mM}$   $\text{Me}_2\text{-ArgTX-636}$ ; lane 14,  $0.8 \text{ mM}$  chlorpromazine.

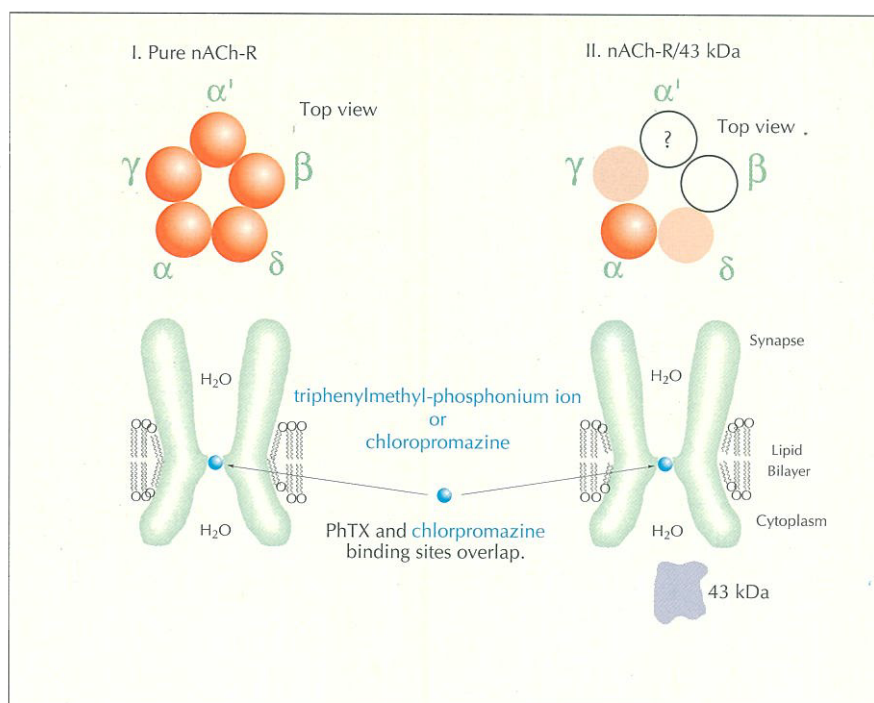
$1.25 \text{ mM}$  cold analog 2 as a competitor reduced binding to 12% of the level observed in the absence of competitor (lane 4). In the presence of a  $1.25 \text{ mM}$  concentration of other nAChR channel blockers, including wasp toxin analogs and a spider toxin analog, all subunits were labeled as in the control, but to a lesser extent due to competition for the binding site: lane 5,  $\text{I}_2\text{PhTX-343-Arg}$ ,  $\sim 0\%$ ; lane 6,  $\text{C10-PhTX-343-Arg}$ ,  $\sim 0\%$ ; lane 7, a spider toxin dimethylargiotoxin-636 [11], 10%; and lane 8, chlorpromazine,  $\sim 0\%$ . The binding site for chlorpromazine is shown schematically in Fig. 6 [22]. The presence of the competitive antagonist  $\alpha$ -bungarotoxin ( $\alpha\text{-BgTX}$ ) which binds to the acetylcholine binding site,

as expected did not appear to affect binding of analog 2 (lane 9). The above results were reproducible with nAChR-rich membranes, in which the receptor channels are embedded in the natural lipid environment, but the receptor-associated 43 kDa protein is removed. Thus in the absence of the 43 kDa protein, all five subunits are uniformly labeled, approximately to the same extent.

#### Crosslinking in the presence of the 43 kDa protein

To examine the influence of the 43 kDa protein on binding, nAChR-rich membranes were purified without adjusting the pH to 11 [29]. Under these conditions the 43 kDa protein is retained, and the  $\alpha$  (and/or  $\alpha'$ ) subunit

**Fig. 6.** Comparison of labeling patterns between nAChR with or without 43 kDa protein. Red designates photocrosslinked subunits. As chlorpromazine inhibits the binding of PhTx analog **2** to nAChR, the binding sites for the two molecules must overlap. The chlorpromazine site is known to be near the gate of the channel from previous studies [22].



was the major labeled component of nAChR cross-linked with analog **2**, whereas  $\gamma$  and  $\delta$  subunits were only weakly labeled (Fig. 5b, lane 11); note that the cytoplasmic protein was also labeled. Other channel blockers such as another PhTX analog, a spider toxin and chlorpromazine competed for binding of analog **2** in the presence of the 43 kDa protein (lanes 12–14). The labeling pattern of the five subunits, with and without the 43 kDa protein, is shown schematically in Fig. 6.

#### Localization of the photoaffinity label by proteolysis

The  $\alpha$  subunit was photoaffinity labeled with analog **2** in the absence of the 43 kDa protein and subjected to proteolytic mapping studies with *Staphylococcus aureus* V8 protease [30–32]. The radioactive label was found predominantly on the 20 kDa fragment comprising Ser173 to Glu338 (Fig. 7a) and, to a much lesser extent, on the 12 kDa peptide, Asn339 to Gly437. In a separate experiment, the labeled  $\alpha$ -subunit was digested with trypsin followed by SDS-PAGE/autoradiography and mass spectroscopy measurements (fast atom bombardment (FAB) and electrospray, JEOL HX/HX110A tandem four-sector mass spectrometer). These studies showed that the peptides linked to the PhTX analog **2** had a molecular weight of less than 2.5 kDa [5]. Since all of the membrane-spanning peptides resulting from trypsin cleavage are expected to have molecular weights of much greater than 2.5 kDa [16], this shows that the azidophenyl moiety does not cross link to moieties inside the membrane-spanning region.

#### Discussion

The photochemical reactivities of the azidophenyl group in analog **2** are expected to be similar to those normally observed with the aryl azide compounds, which have been well-studied [33]. During UV-irradia-

tion (254 nm), analog **2** is electronically excited and loses  $N_2$  from the benzoyl azide group, thus generating the reactive nitrene species. The short-lived nitrene radical can covalently cross-link to any nearby amino acid residue; to our knowledge, the relative activity of various residues, although important, has not been systematically investigated. Nitrenes can also rearrange to dehydroazepines which selectively react with amino acids such as Ser, Thr, Lys and Cys. Certain iodinated aromatic azides containing iodine and the azide group in the same ring are not ideal reagents because they also lose iodine during photolysis, however, a compound containing these groups on separate rings has been shown to retain its iodine during irradiation [34]. We believe that this is also the case for  $N_3Ph-^{125}I_2PhTX-343-Lys$  (analog **2**).

The entire sequence of the nAChR from *Torpedo californica* has been determined [16] and used to predict the structure of the receptor [21,22] (Fig. 8a,b). The pore is lined by the five M2 segments of the subunits of the nAChR which are arranged in such a manner that six five-membered rings, consisting of one side chain from each polypeptide are present. Three of these are anionic (the top and two bottom rings), one is hydrophobic (comprised solely of leucine residues) and the remaining two are hydrophilic. Just below the top anionic ring there is a large hydrophobic space, and the leucine ring forms a constriction near the center of the gate. Also depicted in Fig 8a is the 43 kDa protein that is associated with the cytoplasmic side of the receptor.

Photoaffinity labeling studies have been performed with nAChR using radioactive  $N_3Ph-^{125}I_2PhTX-343-Lys$  (**2**) and the nAChR from *Torpedo californica*. Without the cytosolic 43 kDa protein, all five subunits became linked

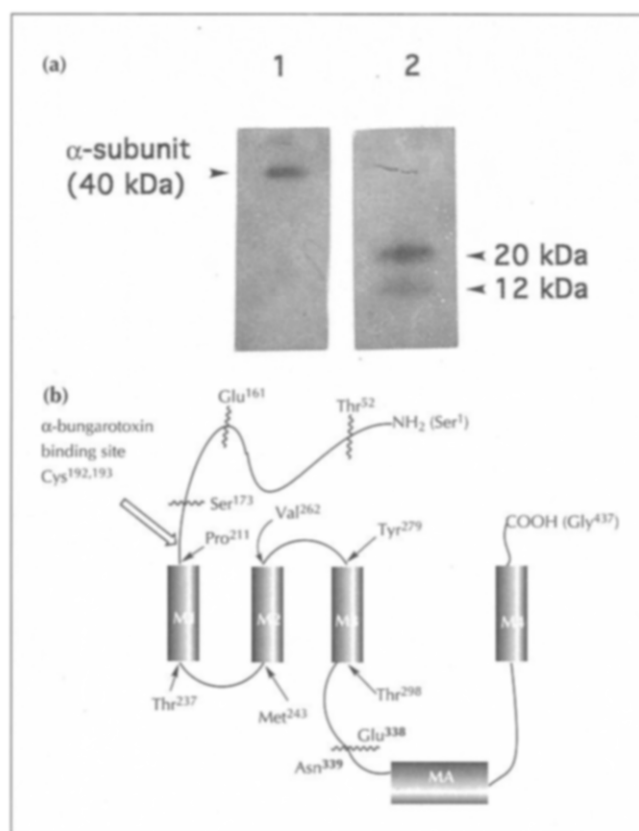


**Fig. 7.** Limited proteolysis of affinity-labeled  $\alpha$ -subunit. **(a)** The  $\alpha$ -subunit from nAChR labeled with analog **2** was proteolyzed to a limited extent with *Staphylococcus aureus* V8 protease according to the method of Cleveland *et al.* [30]. Lanes 1 and 2 are autoradiograms of a mapping gel (15 % polyacrylamide gel): Lane 1, labeled  $\alpha$ -subunit (40 kDa) before proteolysis; Lane 2, radioactive peptide fragments (20 and 12 kDa) after proteolysis. **(b)** Summary of the cleavage positions in V8 limited proteolysis of affinity-labeled  $\alpha$ -subunit. Three major fragments are produced after limited proteolysis: an 18 kDa fragment (Thr52–Glu161), a 20 kDa fragment (Ser173–Glu338) and a 12 kDa fragment (Asn339–Gly437). The 20 kDa fragment is heavily labeled after treatment with analog **2**, the 12 kDa fragment shows some labeling, and the 18 kDa fragment is not labeled. Photolabeling is not affected by  $\alpha$ -BgTX, narrowing the likely area of interaction further.

to the toxin; in contrast, in the presence of the 43 kDa protein, fewer subunits became radioactive, and in addition, the protein itself became crosslinked to analog **2**. Although the interaction of 43 kDa with nAChR is not essential for the channel gating process [19], we propose that the presence or absence of 43 kDa greatly affects the binding of PhTX to the nAChR channel. Thus, the 43 kDa protein may be a useful geometrical marker indicating that the photolabile groups of the toxin analog are oriented toward the cytoplasmic side of the pore. Moreover, the cytosolic protein must be asymmetrically disposed with respect to the nAChR, such that analog **2** preferentially cross-links to the  $\alpha$ -subunit in its presence. Binding of analog **2** to nAChR could be competed for by other potent wasp and spider toxin analogs, indicating that all of these compounds bind to a similar part of the receptor. Binding of analog **2** was also inhibited by chlorpromazine, a non-competitive antagonist of nAChR, which

photocrosslinks to Ser248 of M2 $\alpha$  and to several other residues in the vicinity such as Ser254 of M2 $\beta$ , Thr253 of M2 $\gamma$ , and Ser262 of M2 $\delta$  (see Fig. 8b) [22]. Our data support a model in which the binding of the azidobenzoyl group in analog **2** is sterically directed toward the  $\alpha$  subunit in the presence of the 43 kDa protein, while the polyamine–Lys chain competes with chlorpromazine for the binding site centered around the constricted site within the membrane-spanning ion channel (Fig. 8a).

In the photolabeling studies with analog **2**, the 20 kDa fragment that carried the bulk of the cross-linked sites (Fig. 7) contains the agonist binding site (Cys192–Cys193), transmembrane segment M1 (Pro211–Thr237), M2 (Met243–Val262), M3 (Tyr279–Thr298) and the cytosolic region up to Glu338.  $\alpha$ -BgTX is a competitive antagonist which binds to Cys192/193 [21–23], but did not affect the binding of PhTX analog **2** to the receptor (Fig. 5a). We were able, therefore, to exclude the peptide chains residing close to the  $\alpha$ -BgTX binding site (extracellular chains, Ser173–Pro211 and Val262–Tyr279) from the site of crosslinking in our model. The transmembrane segments M1, M2 and M3 were ruled out as binding sites on the basis of proteolytic studies on the photoaffinity labeled subunit. This leaves the cytoplasmic loops Thr237–Met243 and Thr298–Glu338 as the site(s) of cross linking to analog **2**. The results lead to the proposed model for high-affinity binding of PhTX to nAChR shown in Fig. 8; the conformation of bound state PhTX is extended, and the polyamine chain (regions I/II) and the anchoring groups (regions III/IV) are located in different hydrophilic and hydrophobic sites, respectively.

The alignment shown in Fig. 8 accounts for most of the information summarized in Fig. 2, as detailed below.

### Region I

In this model, it is possible to line the polyamine ammonium moieties of PhTX-433 against the hydrophilic rings, leading to favorable stabilizations from electrostatic and H-bonding interactions. Thus, the relative disposition and the number of protonated groups on the toxin seem to be important in determining the potency. Here, the  $\alpha$ -helical pitch (5.4 Å) matches spacing of the methylenes or their equivalents including the amide bond.

The small differences in activity between PhTX-433 (natural, relative activity 1.0 for nAChR and qGluR), PhTX-343 (0.4 for nAChR and 0.8 for qGluR) and PhTX-334 (1.2 for qGlu-R) presumably arise from subtle differences in the matching between the amino functions of the PhTXs and hydrophilic rings (Fig. 8c). Bu-433 (Fig. 8c), which has a butyl branch from the polyamine chain, surprisingly has an increased potency of 8; the hydrophobic branch probably increases the affinity through hydrophobic binding to Leu251. This can be determined experimentally by photolabeling with an analog carrying the label in this branch. Quaternization of amino groups drastically reduces the activity (the relative activity of per-Me-PhTX-343 is 0.2 for binding to insect

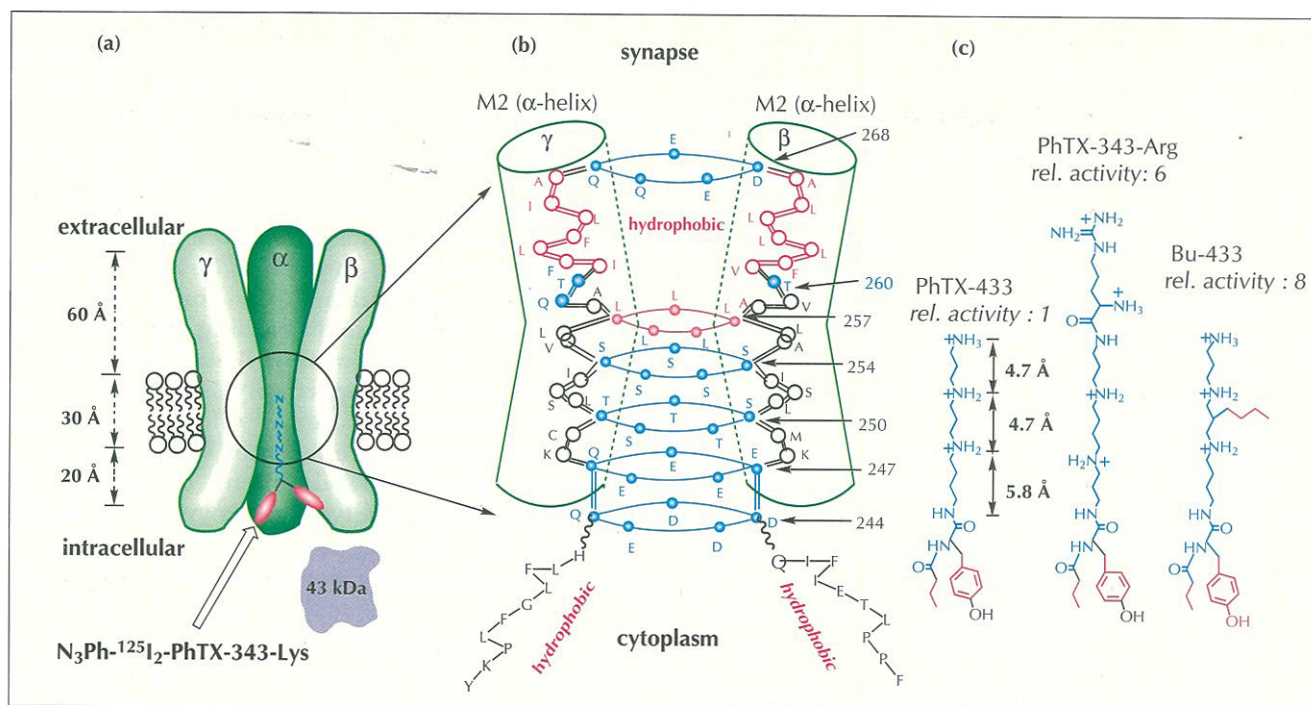


**Fig. 8.** Model of the high-affinity site for philanthotoxin in nAChR. **(a)** Cutaway view of a model for the nAChR with PhTX bound in the gate of the channel. **(b)** Close-up view of the channel gate, with hydrophobic (pink) and hydrophilic (blue) residues shown. **(c)** Structures of PhTX analogs used in this study and elsewhere, with relative activities shown. Philanthotoxin appears to bind on the intracellular face of the pore, with its 'head' oriented outwards and the 'tail' making contact with the hydrophilic internal rings formed by the amphipathic  $\alpha$ -helices of M2. The 'head' region is therefore close to the 43 kDa cytoplasmic protein, consistent with the finding that this protein is labeled in crosslinking studies. The relative activities of the different analogs of PhTX can be rationalized on the basis of the model by proposing that the longer chain of PhTX-343-Arg makes additional hydrogen bonds to the hydrophilic groups lining the channel, and that the butyl group of Bu-433 makes a hydrophobic contact, possibly with Leu251.

qGlu-R), probably because the bulk of the hydrophobic methyl groups hinders hydrogen bond stabilization.

### Region II

The enhanced activity resulting from chain elongation can be rationalized by further H-bonding. For example, the increased activity of PhTX-343-Arg, (Fig. 8c, relative activity = 6), may be due to a hydrogen bond between the terminal guanidinium group and a Thr, possibly Thr260. Electrophysiological and circular dichroic studies using artificial ion channels formed from synthetic M2 peptides embedded in lipid bilayers have unambiguously shown that PhTX interacts with the M2 channel walls [35,36].

### Region III

Activity is enhanced by hydrophobic groups: for example, the activities of the decylamide and benzylamide analogs are four-fold and eight-fold increased over that of PhTX, respectively. Hydrophilic groups such as asparamide reduce activity, however. Regions III and IV probably interact with the hydrophobic amino acid moieties present on the cytoplasmic side of the channel.

### Region IV

Some differences in antagonist activity were observed for binding of analogs with modifications in this region to qGlu-R or nAChR. For binding to qGlu-R, a bulky anchoring group with moderate hydrophobicity appears

to be necessary. The hydroxyl group on Tyr is not required; rather activity is increased in the Phe analog. The systematic change in qGlu-R activity accompanying halogenation of Tyr (8-fold enhancement for  $I_2$ ; 1.5-fold for  $Br_2$ ; no change for  $Cl_2$ ; and 0.5 for F) is noteworthy. It is conceivable that this trend is related to polarization of the molecule during binding. The enhanced activity in the iodinated analog not only leads to enhanced affinity but also allows radiolabeling in the last step in the synthesis [24]. Binding of analogs to nAChR, unlike qGlu-R, is not affected by removal of the bulky aromatic moiety. As might be expected from the circular arrangement of the channel aligning subunits, the affinity is independent of whether the configuration of the Tyr group is *S* or *R*.

Since the nAChRs used in these experiments are randomly oriented in vesicles or in unsealed vesicles (as planar membrane fragments), PhTX could enter the binding site from either the synaptic or cytoplasmic side of the receptor. The photolabeling studies with azidophenyl analog **2** showed that the azido group cross-linked to the cytoplasmic loop and also to the cytoplasmic 43 kDa protein. Thus, at least under the experimental conditions employed, the scheme in Fig. 8 is reasonable.

In the natural system, however, nAChR is embedded in a sealed electrocyte membrane, and therefore only the synaptic entrance would be exposed to applied PhTX.

Thus in the tertiary structure Fig. 8, it may also be possible that the anchoring group of PhTX rests in the hydrophobic pocket, and that the polyamine lies in the hydrophilic gate (an inversion of the configuration of the toxin in Fig. 8a). On the other hand, it has been observed that synthetic PhTX-343 blocks channels gated by insect Glu-R more efficiently and potently when injected into the cytoplasmic region instead of extracellularly [37]. The increased efficiency of cytoplasmic application of a channel blocker has also been noted for the activity of chlorpromazine against a mouse cell line [22]. The model that we are proposing may, therefore, identify the most stable interaction of toxin with receptor if toxin is allowed to enter from either side. It is also possible that, *in vivo*, the hydrophobic end of PhTX may pass through the open gate and reach the cytoplasmic side. Although the working model presented in Fig. 8 is plausible, further mechanistic, kinetic and binding studies are needed. Several studies along these lines, including toxin binding with intact skate electrocytes containing nAChR are in progress.

### Significance

**PhTX-433 and analogs are potent non-competitive, reversible antagonists of various subtypes of glutamate receptors (GluR) and N-acetylcholine receptors (nAChR). There are at least 60 types of polyamine-amide toxins isolated from venomous spider species, which also potently inhibit neurotransmitter receptors by blocking their internal cation-conducting channels [1]. Since wasp and spider polyamine-amide toxins are structurally similar, and since cation channels gated by GluR or nAChR are presumed to share common characteristics in their architecture of channels, it is not surprising to find that their channel blocking activities are relatively nonspecific. It is probable, however, that clarification of the mode of toxin binding to various channel subtypes on a molecular level will eventually lead to potent subtype-specific antagonists. The PhTX analogs are useful tools to investigate the tertiary structures of receptors, ligand-receptor interactions, and the pathway by which the ligands enter and block the open channels, because of the ease with which their elongated structures can be manipulated to allow the attachment of various 'tags' at different points along the length of the molecule.**

**Here, we have used a photolabile analog of PhTX to determine the position and orientation of PhTX binding to the nAChR, in the presence and absence of the 43 kDa cytoplasmic protein. Together with previous results, these results have allowed us to build a model for the interaction of the toxin with the receptor, which proposes that the toxin binds 'head-down' in the gate of the channel, close to the cytoplasmic face. This model can now be tested.**

**The acetylcholine, GABA, glycine and serotonin gated channels are all homologous and belong to one family [21]; the GluRs constitute a separate family, but since modifications in the structure of PhTX have the same effect on GluR binding as they do on nAChR binding, it appears that the GluR gate structures have some similarity to the other ion gated channels. Therefore, a model correctly representing the mode of binding between the PhTX analogs and nAChR should be important in understanding toxin binding for all of these receptors. It is even possible that PhTX analogs with high degrees of specificity for GluRs could be used in affinity isolation of GluRs. The design of antagonists of specific receptor subtypes may be important for the development of therapeutic agents for diseases involving neurological disorders and nerve cell death.**

### Materials and methods

Unless otherwise mentioned, all chemicals and materials were used as received. The wasp/spider polyamine-amide toxins were synthesized according to methods of Choi *et. al.* [11,38] and Goodnow *et. al.* [39]. Frozen electric organs from *Torpedo californica* were purchased from Pacific Bio-marine Lab. Inc., Venice, California.

#### *Preparation of N<sub>3</sub>Ph-PhTX-343-Lys (analog 1) and N<sub>3</sub>Ph-<sup>127</sup>I<sub>2</sub>PhTX-343-Lys (analog 2')*

Analog 1 and 2' were synthesized according to specific procedures as described in Fig. 4 and by the method of Goodnow *et al.* [39]. The non-radioactive iodination of N<sup>3</sup>Ph-PhTX-343-Lys was performed following published procedures [39]. All intermediates and final compounds were characterized by <sup>1</sup>H-NMR, <sup>13</sup>C-NMR and FAB mass spectrometry.

#### *Preparation of N<sub>3</sub>Ph-<sup>125</sup>I<sub>2</sub>PhTX-343-Lys (analog 2)*

To the Nensure vial containing carrier-free 5 mCi of Na<sup>125</sup>I in 14 µl of 10<sup>-5</sup> M NaOH solution, pH 8–10 (Dupont/NEN) were added 80 µl of 1 M K<sub>2</sub>HPO<sub>4</sub> (pH 6.0), 20 µl of 10 mM Na<sup>127</sup>I and 20 µl of 5 mM N<sub>3</sub>Ph-PhTX-343-Lys [36]. After stirring the mixture for 30 s using a small magnetic stirring bar, 26 µl 10 mM chloramine T was added to initiate reaction. The reaction mixture was stirred for an additional 5 min, then 10 µl of 10 mM Na<sub>2</sub>SO<sub>3</sub> was added to quench the reaction. The whole reaction mixture was injected into an analytical reverse-phase HPLC column, by which the product could be purified according to following conditions: (i) column, YMC-ODS (4.0 x 250 mm); (ii) linear gradient, 100 % buffer A (80 % water/20 % MeCN/0.1 % trifluoroacetic acid (TFA)) to 50 % buffer A/ 50 % buffer B (20 % water/80 % MeCN/0.1 % TFA) over 30 min; (iii) flow rate, 2 ml min<sup>-1</sup>; (iv) detection, 274 nm. The 9–11 min fractions corresponding to the desired di-iodo labeled product, the retention time of which was identified by injection of corresponding authentic cold analog, were collected and evaporated to dryness. The residue was solubilized in 1 ml of *Torpedo* saline buffer (250 mM NaCl, 5 mM KCl, 3 mM CaCl<sub>2</sub>, 2 mM MgCl<sub>2</sub>, 5 mM Na<sub>2</sub>HPO<sub>4</sub>, pH 7.0). Typically, starting with 5 mCi of Na<sup>125</sup>I, 2.0 to 3.1 mCi of radiolabeled product was obtained in ~50–62 % radiochemical yield. The chemical conversion yield was almost quantitative.

### Isolation and assay of *Torpedo* nAChR

The nAChR was isolated from electroplaque membranes of *Torpedo californica* rays according to published protocols [25–29]. The affinity purified nAChR (>90–95 % in purity) was prepared by extracting nAChR from crude membranes containing nAChR with soybean lipid/cholate, and by employing *Naja naja*  $\alpha$ -cobrotoxin affinity column (Sigma) chromatography as described [25–27]. The pure nAChR was reconstituted into small unilamellar liposomes according to the published protocol [40]. From reconstituted nAChR, active channel openings were detected in lipid bilayers containing nAChR only after addition of acetylcholine [35]. The nAChR-enriched membrane was obtained after discontinuous sucrose gradient centrifugation of crude membranes [28]. For 43 kDa-extracted nAChR, the above enriched membrane was adjusted to pH 11, followed by shaking for 1 h at 0 °C [29]. The purity of nAChR was estimated with  $\alpha$ -<sup>125</sup>I-BgTX binding assays [26,27,41] and SDS-PAGE according to established protocols [42]. The membranes (1.5–2.0 nmol  $\alpha$ -<sup>125</sup>I-BgTX sites per mg protein) used in these experiments were about 20–30 % in purity of nAChR relative to total protein in the preparation.

### Photocrosslinking experiments

A representative protocol used for photoaffinity labeling experiments follows. The radioactive N<sub>3</sub>Ph-I<sub>2</sub>PhTX-343-Lys (25 Ci mmol<sup>-1</sup>) in *Torpedo* saline was mixed with pure nAChR in 5 mM Tris, pH 7.0 at concentrations of 1.90  $\mu$ M (toxin) and 0.25  $\mu$ M (receptor). After incubation of the mixture for 30 min at 4 °C, carbamylcholine was added to the toxin/receptor at a final concentration of 13  $\mu$ M. The resulting mixture was further incubated for 4 h at 4 °C, followed by 20 min UV-irradiation at 254 nm at 4 °C. After irradiation, the solution was lyophilized and the residue was solubilized in SDS sample loading buffer (0.13 M Tris, 4 % SDS, 3 % DTT, 0.001 % bromophenol blue, pH 6.8) at 2  $\mu$ g protein  $\mu$ l<sup>-1</sup>. When nAChR enriched membranes were used, the irradiated suspension was centrifuged at 14 000 rpm using a small desktop ultracentrifuge, and the pellets were solubilized in sample loading buffer. After centrifugation of SDS sample solution at 14 000 rpm for 5 min, the supernatant was loaded onto gels followed by electrophoresis in a Mini-PROTEAN II Electrophoresis System (Bio-Rad). The SDS polyacrylamide gel was composed of 3 % stacking gel (top 1–2 cm) and 8 % separating gel, the thickness of which was 0.75 or 1 mm. After completion of electrophoresis, gels were fixed in 50 % MeOH/10 % AcOH for 30 min before staining with Coomassie brilliant G in 45 % MeOH/10 % AcOH. For autoradiography, the stained gel was dried, and exposed to X-ray film (Kodak) at –78 °C for 6–12 h with an intensifying screen. The relative intensities of labeling were measured by PhosphorImager®, Molecular Dynamics, in which the dried gel and was kept in a cassette for 4–6 h. Scintillation counting was also used to obtain the cross-linking yield of each lane. Here, each subunit protein band was excised from the wet gel, and each gel slice was suspended in 0.4 ml of 4 % SDS, 10 mM Tris, 20 mM DTT, pH 8.0 in a plastic vial and shaken overnight. The contents of the vial was transferred to a scintillation vial followed by addition of 10 ml scintillation cocktail (Fisher). The radioactivity was measured in a scintillation counter equipped with an I<sup>125</sup> window (Beckman).

### Limited proteolytic mapping studies

Proteolytic mapping of labeled nAChR  $\alpha$ -subunit was performed with *S. aureus* V8 protease according to protocols previously published [30–32]. The nAChR (typically 30  $\mu$ g) labeled with analog **2** was resolved in an 8 % mini slab gel

(0.75 mm thickness) and visualized with Coomassie blue staining. The  $\alpha$ -subunit bands were excised, soaked in overlay buffer (125 mM Tris, 5 % sucrose, 0.1 % SDS, pH 6.8) plus 1 mM dithiothreitol (DTT) for 2 h, and gel slices were transferred to the wells of a mapping gel (1 mm thickness, 5 % stacking and 15 % separating polyacrylamide gel). The *S. aureus* V8 protease (20  $\mu$ l; 0.2 mg ml<sup>-1</sup> overlay buffer) was added to each well followed by 20  $\mu$ l of overlay buffer without DTT. After electrophoretic mapping (70 V for 3.5 h, then 120 V for 3 h) and Coomassie staining, the major radioactive peptide bands (20 and 12 kDa) were detected by autoradiography. For characterization of the radioactive peptides, the wet gel was electroblotted onto Trans-Blot® PVDF membrane (Bio-Rad) followed by partial N-terminal sequencing of the 20 kDa band (Protein Chemistry Core Facility at the Howard Hughes Medical Institute, Columbia University).

**Acknowledgements:** We are grateful to Professor Ron Orlando (then at the Suntory Institute for Bioorganic Research, Osaka; currently at University of Georgia, Athens) for mass spectral measurements. This study has been supported by NIH grant AI-10187 (K.N.), NIH 5 F32-GM-14195-02 (A.K.). K.N. and S.K.C. also acknowledge support from Kanagawa Academy of Science and Technology (KAST) at Columbia University.

### References

1. Usherwood, P.N.R. & Blagbrough, I.S. (1991). Spider toxins affecting glutamate receptors: polyamines in therapeutic neurochemistry. *Pharmacol. Ther.* **52**, 245–268.
2. McCormick, K.D. & Meinwald, J. (1993). Neurotoxic acylpolyamines from spider venoms. *J. Chem. Ecol.* **19**, 2411–2451.
3. Eldefrawi, A.T., *et al.*, & Usherwood, P.N.R. (1988). Structure and synthesis of a potent glutamate receptor antagonist in wasp venom. *Proc. Natl. Acad. Sci. USA* **85**, 4910–4913.
4. Piek, T., *et al.*, & Tong, Y.C. (1988). Polyamine-like toxins — a new class of pesticides? In *Neurotox '88: Molecular Basis of Drug and Pesticide Action*. (Lunt, G.G., ed.), pp. 61–76. Elsevier, Amsterdam.
5. Nakanishi, K., *et al.*, & Usherwood, P.N.R. (1994). Bioorganic studies of transmitter receptors with philanthotoxin analogs. *Pure & Appl. Chem.* **66**, 671–678.
6. Krogsgaard-Larsen, P. & Hansen, J.J., eds (1992). *Excitatory Amino Acid Receptors*. Ellis Horwood Limited, Chichester, England.
7. Ragsdale, D., *et al.*, & Miledi, R. (1989). Inhibition of rat glutamate receptors by philanthotoxin. *J. Pharmacol. Exp. Ther.* **251**, 156–163.
8. Anis, N., *et al.*, & Eldefrawi, M. E. (1990). Structure–activity relationships of philanthotoxin analogs and polyamines on N-methyl-D-aspartate and nicotinic acetylcholine receptors. *J. Pharmacol. Exp. Ther.* **254**, 764–773.
9. Bruce, M., *et al.*, & Usherwood, P.N.R. (1990). Structure–activity relationships of analogues of the wasp toxin philanthotoxin: non-competitive antagonists of quisqualate receptors. *Toxicol.* **28**, 1333–1346.
10. Nakanishi, K., *et al.*, & Eldefrawi, M.E. (1990). Philanthotoxin-433 (PhTX-433), a non-competitive glutamate receptor inhibitor. *Pure & Appl. Chem.* **62**, 1223–1230.
11. Choi, S.-K., Nakanishi, K. & Usherwood, P.N.R. (1993). Synthesis and assay of hybrid analogs of argiotoxin-636 and philanthotoxin-433: glutamate receptor antagonists. *Tetrahedron* **49**, 5777–5890.
12. Brackley, P.T.H., Bell, D., Choi, S.-K., Nakanishi, K. & Usherwood, P.N.R. (1993). Selective antagonism of native and cloned kainate and NMDA receptors by polyamine-containing toxins. *J. Pharmacol. Exp. Ther.* **266**, 1573–1580.
13. Hollman, M., Óshea-Greenfield, A., Rogers, S.W. & Heineman, S. (1989). Cloning by functional expression of a member of the glutamate receptor family. *Nature* **342**, 643–648.
14. Nakanishi, N., Schneider, N.A. & Axel, R. (1990). A family of glutamate receptor genes: evidence for the formation of heteromultimeric receptors with distinct channel properties. *Neuron* **5**, 569–581.
15. Moriyoshi, K., Masu, M., Takahiro, I., Shigemoto, R., Mizuno, N. & Nakanishi, S. (1991). Molecular cloning and characterization of the rat NMDA receptor. *Nature* **354**, 31–37.
16. Noda, M., *et al.*, & Numa, S. (1983). Structural homology of *Torpedo californica* acetylcholine receptor subunits. *Nature* **302**, 528–532.

17. Imoto, K., *et al.*, & Numa, S. (1988). Rings of negatively charged amino acids determine the acetylcholine receptor channel conductance. *Nature* **335**, 645–648.
18. Hucho, F. (1986). The nicotinic acetylcholine receptor and its ion channel. *Eur. J. Biochem.* **158**, 211–226.
19. Maimone, M.M. & Merlie, J.P. (1993). Interaction of the 43 kD postsynaptic protein with all subunits of the muscle nicotinic acetylcholine receptor. *Neuron* **11**, 53–66.
20. Akabas, M.H., Kaufmann, C., Archdeacon, P. & Karlin, A. (1994). Identification of acetylcholine receptor channel-lining residues in the entire M2 segment of the  $\alpha$  subunit. *Neuron* **13**, 919–927.
21. Unwin, N. (1993). Neurotransmitter action: opening of ligand-gated ion channels. *Cell* **72/Neuron** **10**, 31–41.
22. Galzi, J.-L., Revah, F., Besis, A. & Changeux, J.-P. (1991). Functional architecture of the nicotinic acetylcholine receptor: from electric organ to brain. *Annu. Rev. Pharmacol. Toxicol.* **31**, 37–72.
23. Karlin, A. (1993). Structure of nicotinic acetylcholine receptors. *Curr. Opin. Neurobiol.* **3**, 299–309.
24. Goodnow, R.A., *et al.*, & Eldefrawi, M.E. (1991). Synthesis and binding of [ $^{125}$ I]<sub>2</sub>philanthotoxin-343, [ $^{125}$ I]<sub>2</sub>philanthotoxin-343-lysine, and [ $^{125}$ I]<sub>2</sub>philanthotoxin-343-arginine to rat brain membranes. *J. Med. Chem.* **34**, 2389–2394.
25. Eldefrawi, M.E. & Eldefrawi, A.T. (1973). Purification and molecular properties of the acetylcholine receptor from *Torpedo* electroplax. *Arch. Biochem. Biophys.* **159**, 362–373.
26. Hertling-Jaweed, S., Bandini, G. & Hucho, F. (1990). Purification of nicotinic acetylcholine receptors. In *Receptor Biochemistry*. (Hulme, E.C., ed.), pp. 163–176, IRL press, New York.
27. Chak, A. & Karlin, A. (1992). Purification and reconstitution of nicotinic acetylcholine receptor. In *Methods in Enzymology*. (Rudy, B. & Iverson, L.E., eds), pp. 546–555, Academic Press, San Diego.
28. Sobel, A., Weber, M. & Changeux, J. P. (1977). Large-scale purification of the acetylcholine receptor protein in its membrane-bound and detergent-extracted forms from *Torpedo marmorata* electric organ. *Eur. J. Biochem.* **80**, 215–224.
29. Neubig, R.R., Krodell, E.K., Boyd, N.D. & Cohen, J.B. (1979). Acetylcholine and local anesthetic binding to *Torpedo* nicotinic postsynaptic membranes after removal of nonreceptor peptides. *Proc. Natl. Acad. Sci. USA* **76**, 690–694.
30. Cleveland, D.W., Fischer, S.G., Kirschner, M.W. & Laemmli, U.K. (1977). Peptide mapping by limited proteolysis in sodium dodecyl sulfate and analysis by gel electrophoresis. *J. Biol. Chem.* **252**, 1102–1106.
31. Pedersen, S., Dreyer, E.B. & Cohen, J.B. (1986). Location of ligand-binding sites on the nicotinic acetylcholine receptor  $\alpha$ -subunit. *J. Biol. Chem.* **261**, 13735–13743.
32. Blanton, M.P. & Wang, H.H. (1990). Photoaffinity labeling of the *Torpedo californica* nicotinic acetylcholine receptor with an aryl azide derivative of phosphatidylserine. *Biochemistry* **29**, 1186–1194.
33. Turro, N.J. (1978). *Modern Molecular Photochemistry*. The Benjamin Cummings Publishing Co., Inc., Menlo Park.
34. Henriksen, U. & Buchardt, O. (1990). Aryl azides as photolabels. Retention of iodine during photochemical ring expansion of an iodinated tyrosine derivative. *Tetrahedron Lett.* **31**, 2443–2444.
35. Mellor, I.R., *et al.*, & Usherwood, P.N.R. (1995). The effect of the polyamine amide philanthotoxin-343 on nicotinic acetylcholine receptors (nAChR) and nAChR peptides emplaced in lipid bilayers. *Eur. Biophys. J.* in press.
36. Choi, S.-K. (1994). Bioorganic Investigations of polyamine amide toxins and neurotransmitter receptors. PhD Thesis, Columbia University, New York.
37. Brackley, P., Goodnow, R., Nakanishi, K., Sudan, H.L. & Usherwood, P.N.R. (1990). Spermine and philanthotoxin potentiate excitatory amino acid responses of *Xenopus* oocytes injected with rat and chick brain RNA. *Neurosci. Lett.* **114**, 51–56.
38. Choi, S.-K., Goodnow, R.A., Kalivretanos, A., Chiles, G.W., Fushiya, S. & Nakanishi, K. (1992). Synthesis of novel and photolabile philanthotoxin analogs: glutamate receptor antagonists. *Tetrahedron* **48**, 4793–4822.
39. Goodnow, R., *et al.*, & Nakanishi, K. (1990). Synthesis of glutamate receptor antagonist philanthotoxin-433 (PhTX-433) and its analogs. *Tetrahedron* **46**, 3267–3286.
40. Anholt, R., Fredkin, D., Deerinck, T., Ellisman, M., Montal, M. & Lindstrom, J. (1982). Incorporation of acetylcholine receptors into liposomes. *J. Biol. Chem.* **257**, 7122–7134.
41. Schmidt, J. & Raftery, M. A. (1973). A simple assay for the study of solubilized acetylcholine receptors. *Anal. Biochem.* **52**, 349–354.
42. Laemmli, U.K. (1970). Cleavage of structural proteins during the assembly of the head of bacteriophage T4. *Nature* **227**, 680–685.
43. Grishin, E.V., *et al.*, & Federova, I.M. (1986). Structure-functional characterization of argiopine — an ion channel blocker from the venom of spider *Argiope lobata*. *Bioorg. Khim.* **12**, 1121–1124.
44. Grishin, E.V., Volkova, T.M. & Arseniev, A.S. (1989). Isolation and structure analysis of components from venom of the spider *Argiope lobata*. *Toxicon* **27**, 541–549.
45. Adams, M.E., *et al.*, & Venema, V.J. (1987). Structures and biological activities of three synaptic antagonists from orb weaver spider venom. *Biochem. Biophys. Res. Commun.* **148**, 678–683.
46. Aramaki, Y., *et al.*, Nakajima, T. (1986). Chemical characterization of spider toxin, JSTX and NSTX. *Proc. Japan. Acad. (Ser. B)* **62**, 359–362.
47. Jasy, V.J., *et al.*, Volkmann, R.A. (1990). Isolation, structure elucidation, and synthesis of novel hydroxylamine-containing polyamines from the venom of the *Agelenopsis aperta* spider. *J. Am. Chem. Soc.* **112**, 6696–6704.
48. Quistad, G.B., *et al.*, Fu, E.W. (1990). Structures of paralytic acylpolyamines from the spider *Agelenopsis aperta*. *Biochem. Biophys. Res. Commun.* **169**, 51–56.

Received: 16 Aug 1994; revisions requested: 24 Aug 1994; revisions received: 13 Dec 1994. Accepted 22 Dec 1994.